
Aerosol Science and Technology
Publication details, including instructions for authors and subscription information:
http://www.tandfonline.com/loi/uast20

# Crossover from Ballistic to Epstein Diffusion in the Free-Molecular Regime

W. R. Heinson[a], F. Pierce[b], C. M. Sorensen[a] & A. Chakrabarti[a]
[a] Department of Physics, Kansas State University, Manhattan, Kansas, USA
[b] Sandia National Laboratories, Albuquerque, New Mexico, USA
Accepted author version posted online: 21 May 2014.Published online: 21 May 2014.

To cite this article: W. R. Heinson, F. Pierce, C. M. Sorensen & A. Chakrabarti (2014) Crossover from Ballistic to Epstein Diffusion in the Free-Molecular Regime, Aerosol Science and Technology, 48:7, 738-746, DOI: 10.1080/02786826.2014.922677

To link to this article: http://dx.doi.org/10.1080/02786826.2014.922677

*Aerosol Science and Technology*, 48:738–746, 2014

ISSN: 0278-6826 print / 1521-7388 online
DOI: 10.1080/02786826.2014.922677

# Crossover from Ballistic to Epstein Diffusion in the Free-Molecular Regime

**W. R. Heinson,[1] F. Pierce,[2] C. M. Sorensen,[1] and A. Chakrabarti[1]**
[1]*Department of Physics, Kansas State University, Manhattan, Kansas, USA*
[2]*Sandia National Laboratories, Albuquerque, New Mexico, USA*



**We investigate, through simulation, a system of aggregating particles in the free molecular regime that undergoes a crossover from ballistic to diffusive motion. As the aggregates grow, the aggregate mean free path becomes smaller and the motion between collisions becomes more diffusive. From growth kinetics, we find that when the ratio of the aggregate mean path to the mean aggregate nearest neighbor separation reaches of the order of unity, a crossover to diffusive motion occurs. This ratio, called the nearest neighbor Knudsen number, becomes an important parameter in understanding aerosol aggregation in the free molecular regime.**

## 1. INTRODUCTION

From understanding climate change to nanomaterial synthesis, aggregation of aerosol particles is of great importance in both natural phenomena and our technology (Friedlander 1977; Dahneke 1983; Family and Landau 1984; Oh and Sorensen 1997). Aggregation of dispersed aerosol particles can occur under a host of different conditions. In the simplest case, aggregates are formed of approximately the same sized monomers (roughly spherical in shape) that come together under stochastic thermal forces (interactions with the medium) and bind permanently on contact via van der Waals forces. Even within such constraints, a number of particle/medium properties can be varied that highly affect the growth rate, particle morphologies, and resulting cluster size distributions of aggregating systems. In a gaseous medium the pressure, temperature, and molecular mass of the gas are determining factors. The initial particle volume fraction can also be adjusted over a large range, from the very dilute to very dense. The variation of these and other parameters leads to the limiting cases of either ballistic or diffusive type motion of particles between collisions with each other.

All particles dispersed into a medium experience drag forces. If the particles are dispersed in a dense medium, the paths of the medium molecules impinging on the surface of the dispersed particle will be severely affected by those leaving the surface. This produces a "stick" boundary condition at the particle surface in what is known as the *continuum regime* with a continuum, Stokes drag. Stokes drag is inversely proportional to the particle effective mobility radius, which is the geometric radius $a$ if the particle is spherical, and the shear viscosity, which is a continuum property of the medium. If the particles are dispersed in a rarefied medium, the paths of the impinging medium molecules are essentially unaffected by those leaving the particle surface. This produces a "slip" boundary condition at the particle surface in what is known as the *free molecular* regime with an Epstein drag. Epstein drag is inversely proportional to the effective cross sectional area of the particle with a mobility radius squared functionality. The parameter that quantifies the continuum to free molecular regime change is the Knudsen number, $Kn = mfp/a$, where $mfp$ is the mean free path of the medium molecules. When $Kn \to 0$, the continuum regime holds, when $Kn \to \infty$, the free molecular regime holds.

Another important parameter in classifying aggregate motion in a medium is the diffusional Knudsen number $Kn_D$, which is the ratio of the suspended particle's persistence length, $l_a$ to some other characteristic length (the persistence is the stopping distance used to calculate the Stokes number (Kulkarni et al. 2011) when the velocity has the equipartion value). An aggregate's (we shall henceforth consider the suspended particles as aggregates) motion is taken to be on a straight line over a distance equal to its persistence length. When $Kn_D \to \infty$ the persistence length dominates all other length scales and the motion is considered ballistic. When $Kn_D \to 0$ the persistence length is small compared to the system's other length scales and the motion is considered diffusive. The crossover between these two limits occurs when $Kn_D \approx 1$. When the system is *cluster dilute*, the only

Received 30 January 2014; accepted 22 April 2014.
Address correspondence to A. Chakrabarti, Department of Physics, Kansas State University, Manhattan, KS 66506, USA. E-mail: amitc@phys.ksu.edu
Color versions of one or more of the figures in the article can be found online at www.tandfonline.com/uast.

characteristic length scale is the linear size of the aggregate (Pierce et al. 2006). Here, we use a definition of $Kn_D$ similar to that used by Rogak and Flagan (1991) and Gopalakrishnan and Hogan (2011), in the dilute limit

$$Kn_D = \frac{\sqrt{k_B T \mu_{ij}}}{\Gamma_{ij}(R_{g,i} + R_{g,j})} \quad [1]$$

where $k_B$ is the Boltzmann constant, $T$ is temperature, $\mu_{ij}$ is the reduced mass between an aggregate and its collision partner, $R_{g,i}$ is the radius of gyration of the *ith* cluster and $\Gamma_{ij}$ is the reduced drag coefficient between these two aggregates defined as $\Gamma_{ij} = \Gamma_i \Gamma_j / (\Gamma_i + \Gamma_j)$ were $\Gamma_i$ is the drag coefficient of the *ith* cluster. The collision partner for a given cluster is assumed to be its nearest neighbor. This definition of $Kn_D$ is equivalent to the ratio of the collision partners' reduced persistence length to their combined size.

As the system becomes more crowded, the nearest neighbor separation $R_{nn}$ becomes another important length scale (Pierce et al. 2006). If the persistence length of the aggregate $l_a$ is large compared to the nearest neighbor separation then the movement of aggregates between collisions would be on a straight line, that is, ballistic motion. But if $l_a$ is small compared to $R_{nn}$, the aggregate will have to travel many such $l_a$ s, which follow each other randomly, before it collides with another aggregate; then the movement is diffusive. This is illustrated in the Figure 1 where in part (a), the light shaded cluster moves ballistically whereas in part (b) it moves diffusively. With this physical picture in mind, we introduce a new diffusional Knudsen number based on the nearest neighbor separation as a characteristic length scale:

$$Kn_n = \frac{l_a}{R_{nn}} \quad [2]$$

To distinguish it from the traditional diffusional Knudsen number, we will refer this new one as the *nearest neighbor Knudsen number* from here on. (Pierce et al. 2006) We anticipate that the nearest neighbor Knudsen number would be a better descriptor of the crossover from the ballistic to Epstein diffusion as the system becomes *cluster dense* or when the mean persistence length an aggregate travels becomes close to the nearest neighbor distance.

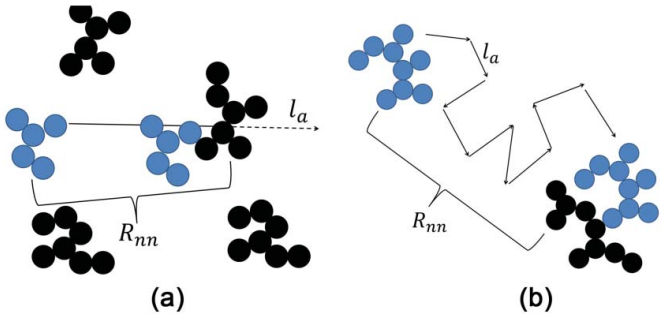


FIG. 1. (a) Illustration of a ballistic collision where the light shaded cluster does not make one full persistence length before colliding with its neighbor. (b) Illustration of a diffusive collision where the light shaded cluster makes several persistence lengths before colliding.

In this article, we present a simulation study of the aggregation of dispersed solid particles in the free molecular regime to demonstrate the effect of crossover between ballistic and Epstein diffusive type motion, a crossover that occurs due to cluster growth. Due to the evolving size of the aggregates or clusters, systems that initially aggregate in a ballistic fashion can cross over to Epstein diffusive as aggregation proceeds. The kinetics of aggregation, resulting cluster size distributions, and aggregate morphologies can all be affected by this crossover, and it is the results of these processes that this article addresses. We use two simulation methods to study this crossover: a direct integration of the Langevin equation (Mountain et al. 1986; Gopalakrishnan and Hogan 2011; Thajudeen et al. 2012) along with a simple and fast Monte Carlo aggregation algorithm that captures the essential physical characteristics of the crossover. The physical realization of this ballistic to diffusive crossover lies, for example, in highly sooting flames.

The rest of the article is organized as follows. In Section 2, we discuss both of our simulation algorithms. In Section 3, we describe the aggregation kinetics and how they are governed by the Smoluchowski equation. Next, Section 4 deals with the scaling of the aggregation kernel and the scaling of the aggregate mass distribution is discussed in Section 5. Results from our simulation studies are given in Section 6 and finally we give our concluding remarks in Section 7.

## 2. SIMULATION METHODS

Two simulation models, Langevin dynamics and Monte Carlo cluster-cluster aggregation, are used in this article. While Langevin dynamics simulations have been used in the past to describe aggregation in the free molecular regime (Nowakowski and Sitarski 1981; Mountain et al. 1986; Mulholland et al. 1988; Ranganathan and Hogan 2011), they are computationally expensive. We have developed a Monte-Carlo (MC) method for the crossover study similar to ones used in the past for continuum regimes (Pierce et al. 2006; Heinson et al. 2010). This MC method has the advantage of being computationally very efficient. Both simulations are constructed so that the crossover from ballistic to Epstein diffusive motion occurs as aggregation proceeded and the aggregate size increased. While the simulations differ in the mechanisms of aggregate movement, they share similar starting points. All simulations start with 100,000 monomers of radius $a$, diameter $\sigma = 2a$ and mass $m_o$ that are placed at random in a 3D simulation box to obtain the desired volume fraction by adjusting the box size. If a monomer placed overlaps with another, it is given new set of random coordinates.

Work presented here was done at volume fraction of $f_v = 10^{-2}, 10^{-3}$, and $10^{-4}$. Periodic boundary conditions are in place to negate edge effects.

### 2.1. Langevin Dynamics

In this part, we integrate the Langevin equation for an aggregate:

$$m_a \ddot{r} = -\Gamma \dot{r} + R(t) \quad [3]$$

where $m_a$ is the aggregate mass, $\Gamma$ is the drag coefficient, $R(t)$ the stochastic thermal force and $r$ the position of a given aggregate center of mass. Aggregate mass can also be written as $m_a = Nm_o$ where $N$ is the number of monomers in an aggregate. The system is set to a constant temperature initially through the assignment of monomer velocities via the Maxwell-Boltzmann distribution. Solving Equation (3) one finds: (Gunsteren and Berendsen 1982)

$$r(t) = T_c \left\{ v(0)\left(1 - e^{-\frac{t}{t_c}}\right) + \int_0^t \left(1 - e^{-\frac{t'-t}{t_c}}\right) \frac{R(t')}{m_a} dt' \right\} \quad [4]$$

Here, the initial aggregate velocity is $v(0)$ and the characteristic time, $t_c = m_a/\Gamma$ is a measure of how long an aggregate will move along a ballistic trajectory before it feels the influence from the medium.

Integration of Equation (4) is done at time steps of $\Delta t = 0.1$ in reduced units of $2a(m_o/k_BT)^{1/2}$. Reduced units of monomer mass $m_o = 1$, monomer radius $a = 0.5$ and $k_BT = 1$ are used to simplify the integration. When two aggregates collide they irreversibly stick, the total number of aggregates $N_c$ is decremented by 1 and the new aggregate moves with a thermal velocity determined by equipartition.

Simulations presented here set out to model aerosol systems at low background gas densities often induced by high temperature and therefore are firmly in the free molecular drag regime. The free molecular drag coefficient is given as

$$\Gamma = 4\pi\delta P \sqrt{\frac{m_g}{3k_bT}} R_m^2 \quad [5]$$

In Equation (5), $\delta$ is the accommodation coefficient, $P$ is pressure, $m_g$ is the mass of a gas medium molecule and $R_m$ is mobility radius of the aggregate. Experiments and previous simulations have shown that the mobility radius for fractal aggregates is

$$R_m = aN^x \quad [6]$$

where the mobility-mass exponent $x = 0.46$ (Wang and Sorensen 1999; Sorensen 2011). Now the drag coefficient becomes

$$\Gamma = 4\pi\delta P \sqrt{\frac{m_g}{3k_bT}} a^2 N^{2x} \quad [7]$$

The ballistic motion persists over a distance given by the product of the characteristic time, $t_c$ and thermal velocity $c = \sqrt{3k_bTm_a}$. Thus, the persistence length is written as

$$l_a = \frac{3k_bT}{4\pi\delta P} \sqrt{\frac{m_0}{m_g}} a^{-2} N^{\frac{1}{2}-2x} \quad [8]$$

Notice that both the drag coefficient and persistence length have a power law dependence on $N$. Setting $N = 1$ yields the monomer persistence length

$$l_0 = \frac{3k_bT}{4\pi\delta P} \sqrt{\frac{m_0}{m_g}} a^{-2} \quad [9]$$

Rescaling Equations (7) and (8) by $l_0$ provide a more compact from of $\Gamma$ and $l_a$

$$\Gamma = \frac{\sqrt{3k_bTm_0}}{l_0} N^{2x} \quad [10]$$

$$l_a = l_0 N^{\frac{1}{2}-2x} \quad [11]$$

From Equation (10) it is clear that $l_0$ and $N$ define the drag coefficient and therefore are necessary to solve the Langevin equation. Thus, $l_0$ along with $f_v$ and number of monomers, become a primary input in the simulation. All $l_0$ values are given are in units of monomer diameter $\sigma$. Values of $l_0 = 1$, 10, 50, 200, 10,000 were used in this work. We will show that when $l_0 = 1$ the system acts as Epstein diffusion while $l_0 =$ 10,000 leads to purely ballistic motion.

### 2.2. Monte Carlo Cluster-Cluster Aggregation

Instead of solving the Langevin equation to move the aggregates, the Monte Carlo CCA method picks an aggregate at random, calculates a probability of movement $P_m$ to determine if the aggregate moves, and then increments time by $1/N_c$ where $N_c$ is the number of aggregates in the system including lone monomers. When the aggregate moves, it travels a distance of one monomer diameter $\sigma$. This model is standard for aerosol Monte-Carlo simulations in the continuum regime, where we differ is how $P_m$ is calculated. In ballistic (BLCA) systems $P_m$ is

proportional to the aggregate velocity and is set as (Pierce et al. 2006)

$$P_{m,B} = N^{-\frac{1}{2}}. \quad [12]$$

For Epstein diffusion the probability of movement is proportional to the aggregate's drag coefficient $\Gamma$ and is set as (Pierce et al. 2006)

$$P_{m,D} = N^{-2x}. \quad [13]$$

Our proposed crossover $P_m$ must let an aggregate move ballistic on the scale of its persistence length $l_a$ and diffusively on length scales larger than $l_a$. Also as an aggregate grows, its persistence length will decrease until $l_a = 1$ via Equation (11). Since in our simulation the minimum step size is one, at the $l_a = 1$ point, $P_m$ must also crossover from ballistic to diffusive. Our proposed $P_m$ is a linear combination of inverse of $P_{m,B}$ and inverse $P_{m,D}$, that is, a harmonic sum of two probabilities.

$$P_m^{-1} = c_1 P_{m,B}^{-1} + c_2 P_{m,D}^{-1} \quad [14]$$

Normalizing so monomers have $P_m = 1$ and crossover happens at $l_a = 1$ Equation (14) becomes

$$P_m^{-1} = \left(1 - \frac{\sigma}{l_0}\right) N^{\frac{1}{2}} + \frac{\sigma}{l_0} N^{2x} \quad [15]$$

where $1 \leq l_o \leq \infty$.

We must note that the procedure for selecting $P_m$ represented in Equation (15) is purely *ad hoc*. However, it captures the physics of the aggregate motion. We will test it by comparing to the Langevin result. Equation (15) determines if an aggregate will move but does not say anything about the direction of movement. Since an aggregate must move on average a distance of $l_a$ before it randomly changes direction due to the influence of the medium molecules, we calculate a probability of random direction change, $P_r$, that is checked every time an aggregate is moved. We chose to use the inverse of $l_a$ for the probability of direction change:

$$P_r = \frac{1}{l_a}. \quad [16]$$

As in Equation (15), $P_r$ is purely *ad hoc* but still captures the physics of the system.

Care must be taken how time is incremented in this hybrid system where a cluster can move either ballistically or diffusively. The time, $\tau_D$ for an aggregate to move one monomer diameter by diffusion is given by the mean square displacement equation $\langle \sigma^2 \rangle = 6\tau_D k_b T/\Gamma$ which yields

$$\tau_D = \sqrt{\frac{m_a}{3k_b T}} \frac{\sigma^2}{2l_a}. \quad [17]$$

Comparing the time to move ballistically one monomer diameter

$$\tau_B = \sigma \sqrt{\frac{m_a}{3k_b T}} \quad [18]$$

to $\tau_D$ and setting $N = 1$ and $l_0 = 1$, the ratio of Equation (17) to Equation (18) is

$$\frac{\tau_{B,0}}{\tau_{D,0}} = \frac{2}{\sigma}. \quad [19]$$

In Monte Carlo simulations a cluster moves a distances of $\sigma$ and time is incremented by $1/N_c$ but when the movement is diffusive the time scale needs to be normalized by Equation (19).

## 3. AGGREGATION KINETICS

The kinetics of aerosol aggregation are governed by the Smoluchowski equation, which describes how the number concentration of clusters of size $N$ monomers, $n_N(t)$, changes with time (Friedlander 1977).

$$\frac{dn_N}{dt} = \sum_{i=1}^{N-1} K(i, N-1) n_i n_{N-1} - n_N \sum_{i=1}^{\infty} K(i, N) n_i \quad [20]$$

The aggregation kernel $K(i,j)$ is the collision rate between aggregates made up of $i$ monomers with aggregates of $j$ monomers. $K(i,j)$ is assumed to be a time-independent homogeneous function of particle size. To simplify the scaling we work under the assumption that the *aggregation is between like-sized clusters,* then the Smoluchowski equation becomes

$$\frac{dn_N}{dt} = -n_N^2 K(N, N). \quad [21]$$

Since $K$ is homogeneous, one can write Equation (21) as

$$\frac{dn_N}{dt} = -n_N^2 N^{\lambda} K(1, 1), \quad [22]$$

where $\lambda$ is the degree of homogeneity, and $K(1,1)$ is the kernel for a monomer–monomer collision. The aggregate size $N$ changes with time and the concentration can be written as,

$$n_N(t) = \frac{n_1(0)}{N(t)} \quad [23]$$

Then Equation (22) becomes

$$N(t)^{-\lambda} dN = K(1, 1) n_1(0) dt. \quad [24]$$

Finally, integration yields

$$N(t) = [1 + (1-\lambda)K(1,1)n_1(0)t]^{\frac{1}{1-\lambda}} \quad [25]$$

or

$$N(t) \approx [t_0 + t]^z \quad [26]$$

with a kinetic exponent, $z$ as first seen by van Dongen and Ernst

$$z = \frac{1}{1-\lambda} \quad [27]$$

and

$$t_0 = \frac{z}{K(1,1)n_1(0)}. \quad [28]$$

Expanding Equation (26) for small time $t < t_0$ one finds that $N(t) \propto t$. After this, small transient time, there is a transition when $t \approx t_o$, and then ultimately at large time when $t > t_0$, the cluster size increases with power law $N(t) \propto t^z$. If the crossover happens during the linear transient regime, then information about the homogeneity will be absent. To avoid this below we simply graph average aggregate size $\overline{N}(t)$ versus $t_0 = t$; a process that by Equation (26) linearizes a double logarithmic graph.

## 4. SCALING ANALYSIS OF THE AGGREGATION KERNEL

The previous section discussed how aggregation governed by the Smoluchowski equation yielded an average cluster size that increased with time via a power law with the kinetic exponent. Here, we present a simple scaling analysis that describes how the collision kernel and its homogeneity determine the kinetics for different regimes of motion. Beginning with the general statement that $K$ is proportional to the colliding particles relative collision cross-sectional area, $A$ and relative velocity, $v$, we write

$$K \sim Av. \quad [29]$$

### 4.1. Ballistic Regime

In the ballistic regime velocity is $v \sim N^{-1/2}$ due to equipartition of energy and since $R_g \sim N^{1/D_f}$ one finds from Equation (29):

$$\lambda_{\text{ballistic}} = \frac{2}{D_f} - \frac{1}{2} \quad [30]$$

Using the accepted value of fractal dimension, $D_f = 1.9$, in the ballistic limit (Fry 2003), the homogeneity is found to be $\lambda_{\text{ballistic}} = 0.55$ and via Equation (30), hence the kinetic exponent is $z_{\text{ballistic}} = 2.2$.

### 4.2. Epstein Diffusion Regime

In the diffusion regime, the characteristic velocity is $v \sim (\Gamma R_c)^{-1}$, where $R_c$ is a characteristic diffusional length scale. In the dilute limit, the only length scale is $R_c = R_g$ and from Equation (29) one finds the homogeneity as

$$\lambda_{\text{Epstein;dilute}} = \frac{1}{D_f} - 2x. \quad [31]$$

Aggregates in the Epstein diffusion regime have a fractal dimension of $D_f = 1.8$ which yields $\lambda_{\text{Epstein;dilute}} = -0.36$ and $z_{\text{Epstein;dilute}} = 0.73$. As the system becomes more crowded the relevant length scale becomes $R_c = R_{nn}$. The nearest-neighbor separation is $R_{nn} \sim N_c$ where $N_c$ is the number of clusters in the system. The total number of monomers, $N_m$ is constant and equals $N_m = N_c - N$, thus $R_{nn} \sim -N^{1/3}$ and the homogeneity is

$$\lambda_{\text{Epstein;dilute}} = \frac{2}{D_f} - \frac{1}{3} - 2x. \quad [32]$$

In the Epstein limit, as the system becomes crowded, then, by Equation (32) homogeneity is $\lambda_{\text{Epstein;dilute}} = -0.14$ and the kinetic exponent is $z_{\text{Epstein;dilute}} = 0.88$.

## 5. SCALING ANALYSIS OF THE CLUSTER SIZE DISTRIBUTION

As aggregation proceeds in the system, the aggregate size distribution develops a scaling form given by $n(N)S^2 = M_1\varphi(x)$ where $n(N)$ is the number concentration of aggregates of size $N$, $M_1$ is the 1st moment of the size distribution and $s$ is the average size (van Dongen and Ernst 1985). The scaling variable is $x = N/S$ and the scaled distribution function, $\supset(x)$ has the form $\varphi(x) = Ax^{-\lambda}e^{-(1-\lambda)x}$ for large sizes ($x > 1$) (Oh and Sorensen 1997). Thus,

$$n(N)s^2 = M_1 Ax^{-\lambda}e^{-(1-\lambda)x} \quad [33]$$

## 6. RESULTS

The aggregation kinetics for both Brownian dynamics and Monte Carlo simulations are shown in Figures 2a–f. The graphs shown the inverse number of clusters $N_c^{-1}$ versus $t + t_0$ for various $l_0$'s. Since the number monomers remains constant, $N_c^{-1}$ is directly proportional to average cluster size. The constant $t_0$ was calculated by Equation (28). The monomer aggregation kernel $K(1,1)$ and $z$ used in Equation (28) were decided based on the initial $Kn_D$ and $Kn_n$. Diffusive and

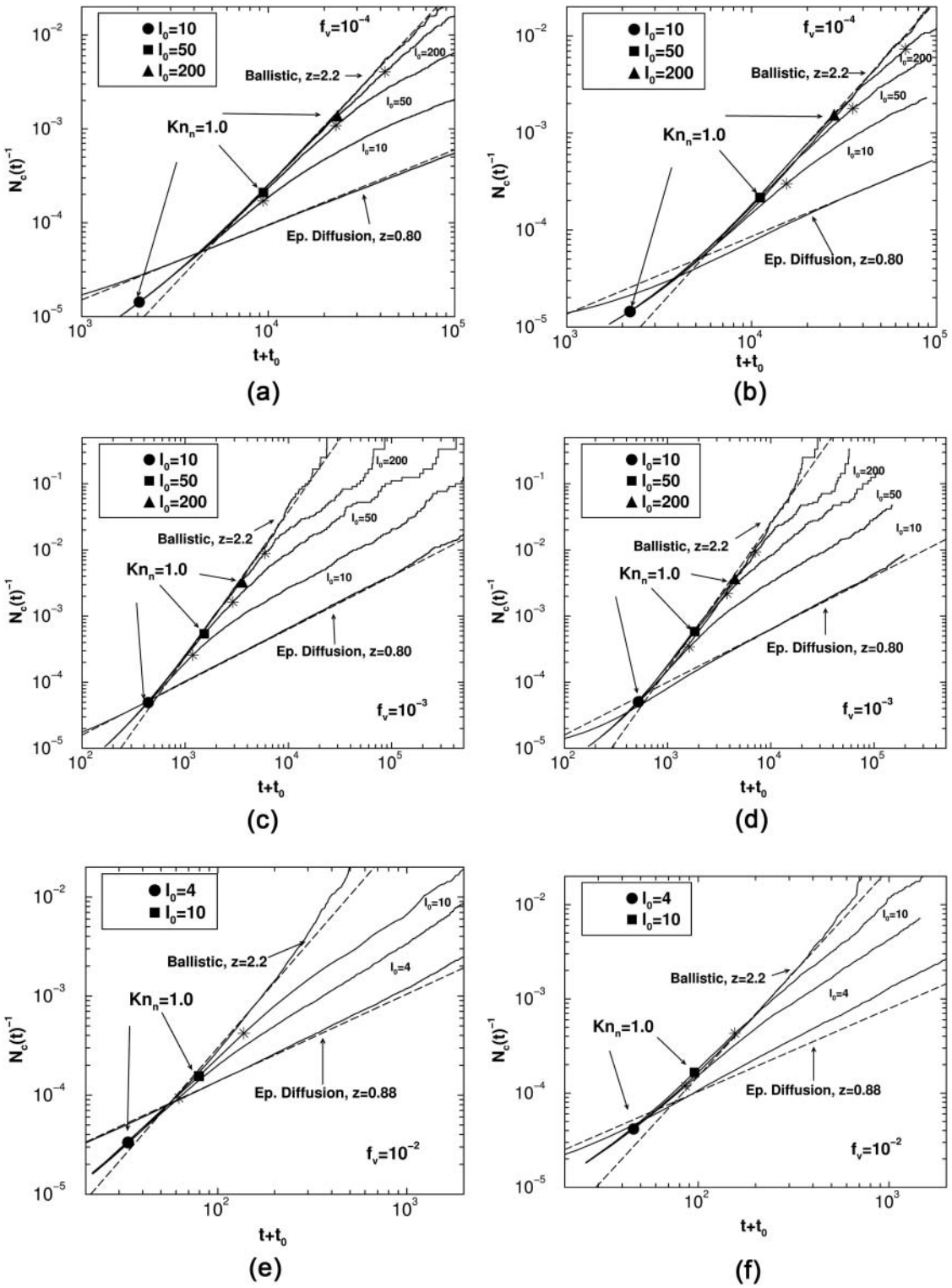


FIG. 2. Inverse cluster count versus $t + t_0$. $t_0$ was found from Equation (28). The lower dashed guide line has a kinetic exponent $z = 0.80 - 0.88$ and the upper guide line has $z = 2.2$. The points where $Kn_n = 1$ are marked and noted in the legend. The points where $Kn_d = 1$ are noted as stars in their respective runs. (a) Monte Carlo simulation at $f_v = 10^{-4}$; (b) Brownian Dynamics simulation at $f_v = 10^{-4}$; (c) Monte Carlo simulation at $f_v = 10^{-3}$; (d) Brownian Dynamics simulation at $f_v = 10^{-3}$; (e) Monte Carlo simulation at $f_v = 10^{-2}$; (f) Brownian Dynamics simulation at $f_v = 10^{-2}$. Notice that in (e) and (f) the Epstein diffusion exponent is $z = 0.88$ as expected when in the cluster dense regime. Also of note in (e) and (f) the trend has upward curvature do to the onset of gelation.

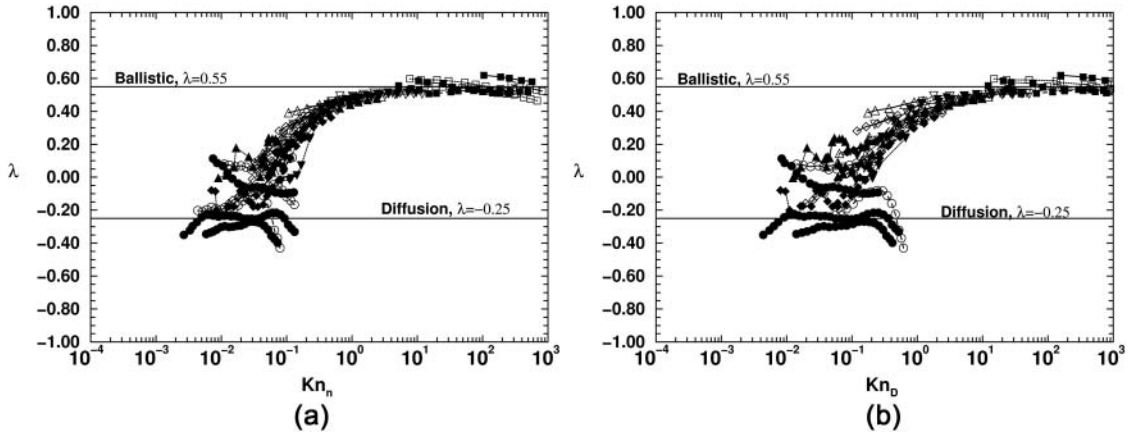


FIG. 3. (a) Aggregation kernel homogeneity $\lambda$ versus nearest neighbor Knudsen number $Kn_n$ for all Monte Carlo and Brownian Dynamic simulations. (b) The diffusive Knudsen number $Kn_D$ versus homogeneity $\lambda$ for all Monte Carlo and Brownian Dynamic simulations. Both measurements show similar behavior and provide a means of detecting the crossover.



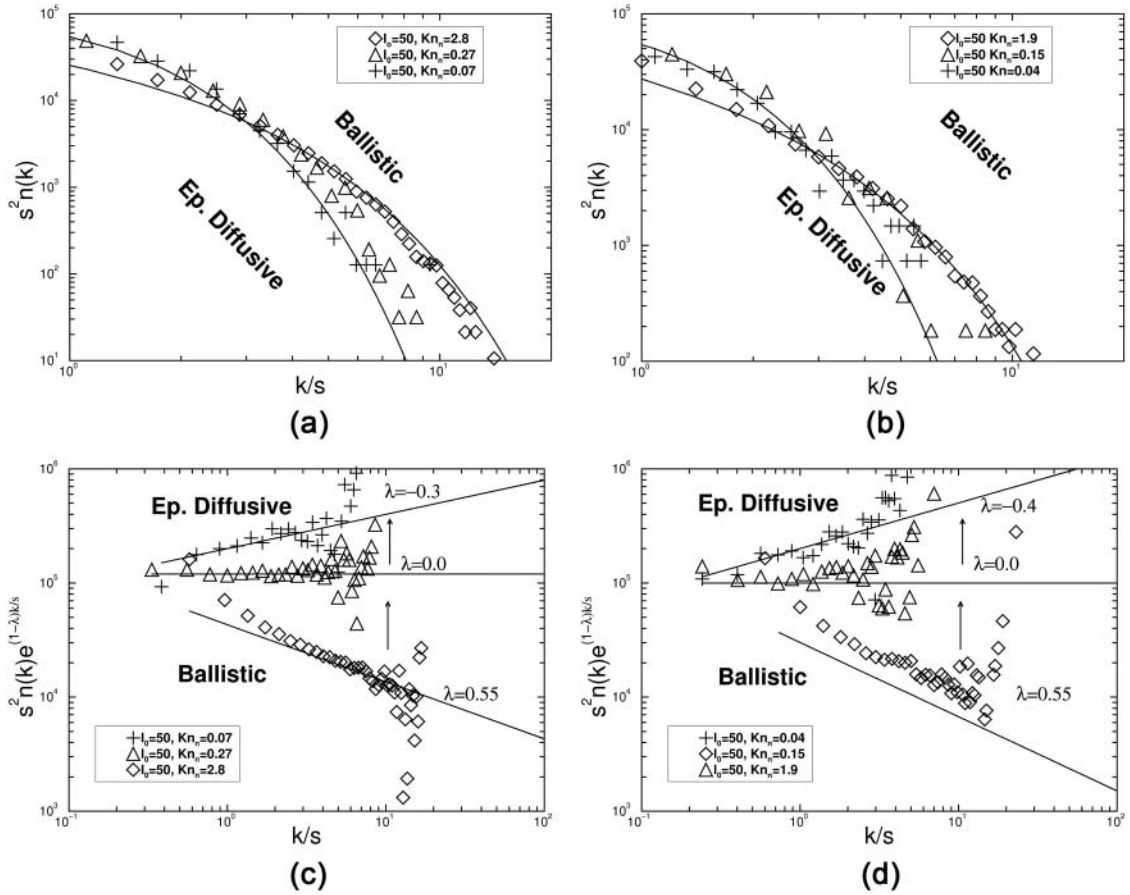


FIG. 4. Aggregate size distribution from Brownian Dynamics with $l_0 = 50$ and $f_v = 10^{-3}$. Lines represent fits from Equation (33). The system starts off with ballistic $\lambda$ then enters an intermediate regime during the crossover and finally at late time and small $Kn_n$ reaches a diffusive $\lambda$. (a) Size distribution from Monte Carlo simulations; (b) size distribution from Brownian Dynamics simulations; (c) rescaled data from (a), here the homogeneity $\lambda$ transition from ballistic to diffusive can be clearly seen. The system starts with ballistic homogeneity of $\lambda = 0.55 \pm 0.1$ then changes to $\lambda = -0.3 \pm 0.2$, consistent to other values of $\lambda$ reported for Epstein diffusion. (d) Rescaled data from (b), the system starts with ballistic homogeneity of $\lambda = 0.55 \pm 0.1$ then changes to $\lambda = -0.40 \pm 0.2$, consistent with Epstein diffusion.

nearest neighbor Knudsen numbers were found for each aggregate by Equations (1) and (2), respectively, then averaged to obtain $Kn_D$ and $Kn_n$ for the system. For runs with $l_0 = 1$ both $Kn_D$ and $Kn_n$ were less than unity and firmly in the diffusive regime, so values of diffusive $K(1,1)$ and $z$ were used. All other runs started with larger $Kn_D$ and $Kn_b$ and therefore ballistic values of $K(1,1)$ and $z$ were used to find $t_0$. When $l_0$ =1, the system is entirely diffusive due to both $Kn_D$ and $Kn_n$ being less than unity and yields a kinetic exponent of $z = 0.8$ for $f_v = 10^{-3}$ and $10^{-4}$ and $z = 0.88$ for the dense $f_v = 10^{-2}$. Both these values are consistent with predicted values of $z = 0.73$ for dilute Epstein diffusion and $z = 0.88$ for dense Epstein diffusion, respectively (Pierce et al. 2006).

At large $l_0$, Figure 2's parts all show for both types of simulation a kinetic exponent of $z = 2.2$ as expected for ballistic motion at all $f_v$ (Pierce et al. 2006). The intermediate values of $l_0$ initially follow the ballistic track then evolve to the diffusive $z$ exponents. For all intermediate $l_0$ runs, the places where $Kn_D = 1$ are marked by a star and places where $Kn_n = 1$ are marked by symbols. While both Knudsen numbers fall within the crossover $Kn_n$ does a better job of marking the beginning of the transition.

Figure 3 plots the aggregation kernel homogeneity $\lambda$ versus either diffusional Knudsen number. By numerically finding $z$ from the data in Figure 2 and using Equation (27) to find $\lambda$, we compare $Kn_n$ to $\lambda$ in Figure 3a and $Kn_D$ to $\lambda$ in Figure 3b. Closed symbols represent data from Monte Carlo simulations and open symbols are data from Brownian dynamics. All runs follow the same trend with a ballistic like upper limit of $\lambda = 0.55$ and an Epstein diffusional lower limit between $\lambda = -0.36$ for cluster dilute systems with $f_v = 10^{-4}$, $10^{-3}$ and $\lambda = -0.14$ for cluster dense systems with $f_v = 10^{-2}$. A crossover present when either Knudsen number is in the 0.1 to 10 range.

In Figures 4a and b the size distributions at different times for the system at $l_0 = 50$ and $f_v = 10^{-3}$ are shown for Brownian Dynamics and Monte Carlo simulations, respectively. The homogeneity is found from fitting Equation (33). At early times when $Kn_n > 1$, the homogeneity is $\lambda = 0.55 \pm 0.1$ consistent with ballistic motion, and at late time when $Kn_n < 1$, the system moves to $\lambda = -0.4 \pm 0.2$ for the Brownian Dynamics runs and to $\lambda = -0.3 \pm 0.2$ for the Monte Carlo runs, both of which are in the range of previous reported values of $\lambda = -0.36$ to $-0.14$ for Epstein diffusion (Pierce et al. 2006). The transition of $\lambda$ can be seen more clearly by scaling Equation (33) by $e^{(1-\lambda)x}$. Figures 4c and d show the rescaled mass distributions at different $Kn_n$ values for runs of $l_0 = 50$. Again as in Figures 4a and b, $\lambda$ moves from a ballistic value to diffusive with changing $Kn_n$.

## 7. CONCLUDING REMARKS

We have performed simulations of the common yet previously unexplored aerosol situation in which the motion of the aggregates transforms from ballistic to Epstein diffusive while in the Free Molecular regime. Two algorithms were used. First, a slow but rigorous Brownian Dynamics method that solved for aggregate motion through the integration of the Langevin equation. Second, a less exact but faster Monte Carlo method that decides aggregate movement through use of an *ad hoc* probability of movement and probability of random walk. The probability of movement is a combination of the well-established probability of movements from ballistic and diffusive simulations and a probability of random walk insures aggregates on average move in a ballistic a distance of $l_a$. All simulations over all $l'_0 S$ produced fractal aggregates of dimension 1.8 except for the very large $l_0 = 10{,}000$ that yielded fractal dimension of 1.9. Both systems were in good agreement with regard to the time evolution of the nearest-neighbor and diffusion Knudsen number.

Volume fractions used went from the light $f_v = 10^{-4}$ to a dense $f_v = 10^{-2}$ to highlight the importance of $R_{nn}$ as the dominant length scale in dense systems. To our surprise we found that at all volume fractions studied both nearest-neighbor separation and aggregate size were equally adequate at describing the crossover. In the future, simulations must be done with both denser and lighter systems to determine if both length scales do indeed remain markers of aggregation kinetics.

One physical situation in which the results of this article would apply is dense high temperature aerosols. Consider, for example, air at STP with a mean free path of 66 *nm* which means monomers of radius $a = 10$ *nm* would experience Epstein drag. Using an accommodation coefficient of $\delta = 1.36$ for $N_2$ gas yields by Equation (9) $l_0 = 30$ nm. If these monomers had a volume fraction of $f_v = 10^{-6}$ then one finds $Kn_n = 0.03$, placing the system in the Epstein diffusion regime. As the aggregates grow from these initial conditions, the system would move to the continuum regime which is not accounted for in our simulations. Raising the temperature to that of typical flame experiments, $T = 2100$ *K*, the persistence length of the monomers grows to $l_0 = 210$ nm yielding a $Kn_n = 0.21$, placing the system in the crossover regime between ballistic and diffusive motion, see Figure 3. Raising the volume fraction in the flame to $f_v = 10^{-4}$ lowers the nearest neighbor separation which in turn gives a $Kn_n = 1.00$, in the middle of the ballistic to diffusive crossover. These latter conditions have been studied experimentally in the past 15 years (Sorensen et al. 1998, 2003; Kim et al. 2004, 2006; Chakrabarty et al. 2012). Finally, we remark that the reverse crossover from diffusive to ballistic aggregation can occur in dense systems near the gel point (Sorensen and Chakrabarti 2011).

## FUNDING

This material is based upon work supported by the National Science Foundation under grant no. AGS 1261651.

## REFERENCE


Chakrabarty, R. K., Moosmuller, H., Garro, M. A., and Stipe, C. B. (2012). Observation of Superaggregates from a Reversed Gravity Low-Sooting Flame. *Aerosol Sci. Technol.,* 46:I–Iii, doi:10.1080/02786826.2011.608389.

Dahneke, B. (1983). Simple Kinetic Theory of Brownian Diffusion in Vapors and Aerosols, in *Theory of Dispersed Multiphase Flow*, R. E. Meyer, ed., Academic Press, New York, pp. 97–134.

Family, F., and Landau, D. P., (1984). *Kinetics of Aggregation, and Gelation.* North-Holland, and Elsevier, Amsterdam.

Friedlander, S. K. (1977). *Smoke, Dust, and Haze: Fundamentals of Aerosol Dynamics*. Wiley, Oxford University Press, New York.

Fry, D., (2003). *Aggregation in Dense Particulate Systems* (PhD diss.). Kansas State University.

Fuchs, N. A. (1964). *The Mechanics of Aerosols*. Dover Publications.

Gopalakrishnan, R., and Hogan, C. J. (2011) "Determination of the Transition Regime Collision Kernel from Mean First Passage Times. *Aerosol Sci. Tech.,* 45:1499–1509.

Gunsteren, W. F., and Berendsen, H. J. C. (1982) Algorithms for Brownian Dynamics. *Mol. Phys.,* 45:637–647.

Heinson, W. R., Sorensen, C. M., and Chakrabarti, A. (2010). Does Shape Anisotropy Control the Fractal Dimension in Diffusion-Limited Cluster-Cluster Aggregation? *Aerosol Sci. Tech.,* 44:I–IV.

Kim, W. G., Sorensen, C. M., and Chakrabarti, A. (2004). Universal Occurrence of Soot Aggregates with a Fractal Dimension of 2.6 in Heavily Sooting Laminar Diffusion Flames. *Langmuir* 20:3969–3973.

Kim, W.G., Sorensen, C. M., Fry, D., and Amit Chakrabarti (2006). Soot Aggregates, Superaggregates and Gel-Like Networks in Laminar Diffusion Flames. *J. Aerosol Sci.,* 37:386–401.

Kulkarni, P., Baron, P. A., and Willeke, K. (2011) Fundamentals of Single Particle Transport, in *Aerosol Measurement Principles, Techniques and Applications*, P. Kulkarni, P. A. Baron, K. Willeke, eds., Wiley, Hoboken.

Mountain, R. D., Mulholland, G. W., and Baum, H. (1986). Simulation of Aerosol Agglomeration in the Free Molecular and Continuum Flow Regimes. *J. Coll. Interface Sci.,* 114:67–81.

Mulholland, G. W., Samson, R. D., Mountain, R. D, and Ernst, M. H. (1988). Cluster Size Distribution for Free Molecular Agglomeration. *Energy Fuels,* 2:481–486.

Nowakowski, B., and Sitarski, M. (1981). Brownian Coagulation of Aerosol Particles by Monte Carlo simulation. *J. Coll. Interface Sci.,* 83:2196–2203.

Oh, C., and Sorensen, C. M. (1997). Light Scattering Study of Fractal Cluster Aggregation Near the Free Molecular Regime. *J. Aerosol Sci.,* 28:937–957.

Pierce, F., Sorensen, C. M., and Chakrabarti, A. (2006). Computer Simulation of Diffusion-Limited Cluster-Cluster Aggregation with an Epstein Drag Force. *Phys. Rev. E,* 74:021411-1-021411-8.

Rogak, S. N, and Flagan, R. C. (1991). Coagulation of Aerosol Agglomerates in the Transition Regime. *J. Colloid Interface Sci.,* 151:203–221.

Sorensen, C. M. (2011). The Mobility of Fractal Aggregates: A Review. *Aerosol Sci. Tech.,* 45:755–769.

Sorensen, C. M., and Chakrabarti, A. (2011). The Sol to Gel Transition in Irreversible Particulate Systems. *Soft Matter,* 7:2284–2296.

Sorensen, C. M., Hageman, W. B., Rush, T. J., Huang, H., and Oh, C. (1998). Aerogelation in a Flame Soot Aerosol. *Phys. Rev. Lett.,* 80:1782–1785.

Sorensen, C. M., Kim, W., Fry, D., Chakrabarti, A. (2003). Observation of Soot Superaggregates with a Fractal Dimension of 2.6 in Laminar Acetylene/Air Diffusion Flames. *Langmuir* 19: 7560–7563.

Thajudeen, T., Ranganathan, G., and Hogan, C. J. (2012). The Collision Rate of Nonspherical Particles and Aggregates for all Diffusive Knudsen Numbers. *Aerosol Sci. Tech.,* 46:1174–1186.

van Dongen, P. G. J., and Ernst, M. H. (1985). Dynamic Scaling in the Kinetics of Clustering. *Phys. Rev. Lett.,* 54:1396–1399.

Wang, G. M., and Sorensen, C. M. (1999). Diffusive Mobility of Fractal Aggregates Over the Entire Knudsen Number Range. *Phys. Rev. E,* 60:3036–3044